

## FIRE SHAPES AND THE ADEQUACY OF FIRE-SPREAD MODELS

D.G. GREEN <sup>1</sup>, A.M. GILL <sup>2</sup> and I.R. NOBLE <sup>3</sup>

<sup>1</sup> *Department of Biogeography and Geomorphology, A.N.U., P.O. Box 4, Canberra, A.C.T. 2601 (Australia)*

<sup>2</sup> *Division of Plant Industry, C.S.I.R.O., P.O. Box 1600, Canberra, A.C.T. 2601 (Australia)*

<sup>3</sup> *Research School of Biological Science, A.N.U., P.O. Box 475, Canberra, A.C.T. 2601 (Australia)*

(Accepted for publication 30 March 1983)

### ABSTRACT

Green, D.G., Gill, A.M. and Noble, I.R., 1983. Fire shapes and the adequacy of fire-spread models. *Ecol. Modelling*, 20: 33–45.

It has been suggested that shapes of burned areas resulting from fires spreading under uniform fuel and meteorological conditions may be described as ellipses, double ellipses, or ovoids. The adequacy of these shapes (together with simulation outputs) as bases for fire spread models was tested by finding the best fits of each shape to maps of experimental fires and comparing the results with fits given by a rectangle (an unlikely fire shape). Each of the models (ellipse, double ellipse, ovoid, simulation model, and even the rectangle) provided adequate approximations to the fire contours used in the tests. The parameter trends found implied that the fires examined tended to become more nearly elliptical in shape and to have higher eccentricity as they grew.

### INTRODUCTION

There are many practical benefits in being able to predict patterns of fire spread through vegetation. Much fire research has therefore been concerned with fire spread and its prediction using models presented as circular slide rules, tables, or sets of equations suitable for machine processing (in eastern Australia: McArthur, 1962, 1966 and Noble et al., 1980; in Western Australia: Sneeuwjagt and Peet, 1979; in U.S.A.: Rothermel, 1972).

Most fire-spread models predict forward rate of spread only. To predict actual areas burned in fires it is necessary to understand fire shapes. A number of researchers have assumed that fire shapes tend to be simple ellipses (Van Wagner, 1969) or double ellipses (Albini, 1976). The validity of these assumptions has never been tested. Only Peet (1967) has measured

experimental shapes and reported on the data. He concluded that an egg-shape (that is an “ovoid”, a variant on the ellipse) is the most appropriate model for mild fires in Western Australian *Eucalyptus* forest.

In this study we set out to test the relative adequacy of various models of the shapes of small test fires in grassy and eucalypt fuels. We include a simulation model pertinent to discrete fuel types and test whether the models considered are more adequate than a rectangle, an extreme and unlikely model upon which to base predictions of spread for landscape fires. Because literature on curve-fitting of geometric shapes is scant, we describe the mathematics used in some detail.

## MODEL ADEQUACY

Many factors influence fire shape, and most of the factors can vary considerably in any real fire, so it is unlikely that the assumptions underlying any fire spread model are ever perfectly satisfied in the real world. Most fire-spread models assume uniform, continuous fuel, uniform wind velocity throughout the burning area, and flat terrain. These assumptions are not always valid. For instance the assumption of uniform wind velocity often fails, especially for widespread, intense fires that affect air movement. Prevailing wind velocity itself is usually highly variable, both in space and through time.

The most important practical question to ask, therefore, is how adequate a model is to describe real fire shapes. At the very least, the parameters used to fix a model should correlate with environmental variables, such as prevailing windspeed, since the model is otherwise non-predictive and therefore useless. Furthermore, an adequate model should give better approximations to real fire shapes than some arbitrary and unlikely shape such as a rectangle. If one model gives consistently better fits to realized fire shapes than a second model, then the first model is clearly the more adequate of the two.

## MODELS OF FIRE SHAPE

### *The elliptical model*

Van Wagner (1969) has assumed that a fire spreading from a point source forms an ellipse, but with the ignition point not necessarily as focus (Fig. 1b). The eccentricity of the ellipse increases as a function of windspeed and its rate of growth is a function of windspeed and fire intensity. These patterns can serve as the basis for fire spread models (Anderson et al., 1982).

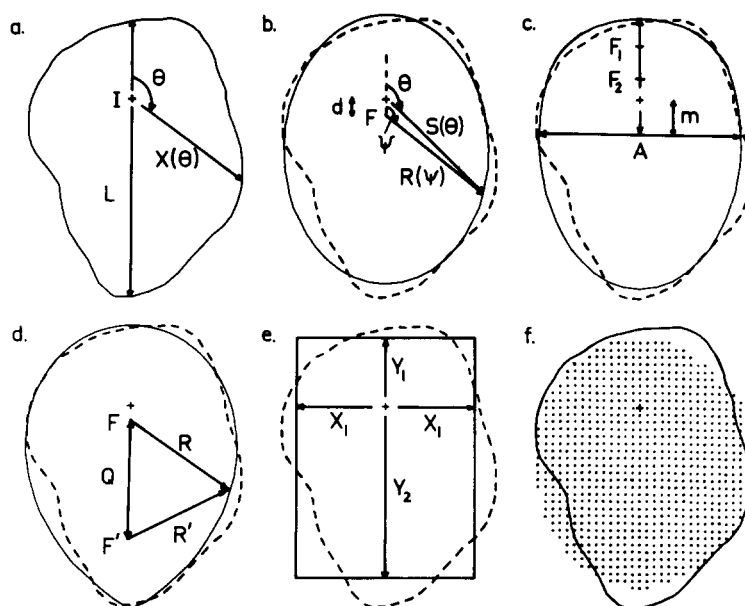


Fig. 1. Map of the boundary of an experimental fire (a) and best fits to it of (b) an ellipse, (c) a double ellipse, (d) an ovoid, (e) a rectangle, and (f) a simulation model. The prevailing wind direction was down the page. In (a) the locations of the fire boundary at other times during the experimental burn are not shown. On each diagram a cross denotes the ignition point of the experimental fire. The symbols indicate points and parameters used in model fitting; see the text for their explanation. The fire boundary is shown as a dashed line in (b)–(e). The dots in (f) indicate ignited fuel in the simulation.

### *The double ellipse model*

Numerous studies (Albini, 1976) have produced equations for rates of fire spread downwind (headfire), and upwind (backfire). Headfire and backfire rates of spread have often been found to be inconsistent with predictions of an elliptical fire-spread model.

The double ellipse model (Albini, 1976) assumes that overall fire shape is given approximately by two ellipses interlocking across a common minor axis (marked by A in Fig. 1c). The first ellipse models the spread of the backfire, while the second models the spread of the headfire. The ignition point does not necessarily coincide with the focus of either ellipse.

### *The ovoid model*

Relationships between headfire and flankfire rates of spread in eucalypt litter led Peet (1967) to suggest that overall fire shapes may be ovoids

(egg-shapes). An ovoid (Fig. 1d) is a generalized ellipse defined by the property that the distances  $R$  and  $R'$  of any point on the curve from two foci  $F$  and  $F'$  satisfy the equation:

$$aR + bR' = k, \quad (1)$$

where  $a$ ,  $b$ , and  $k$  are constants that determine the exact shape of the ovoid (Sussman, 1966); in the special case where  $a = b$ , an ellipse is generated.

### *The discrete fuel model*

Many grass, shrub and crown fires, do not have continuous fuel beds, yet the effects of discrete fuel distribution on fire spread have been largely ignored (exceptions include Kourtz and O'Regan, 1971; Frandsen, 1974; Valendik et al., 1977; Frandsen and Andrews, 1979). The model used in this study is described fully in Green (1983) and incorporates the discrete nature of horizontal fuel packing to simulate fire-spread (Fig. 1f). Fuel is represented by points in a rectangular grid and the spread of a fire is simulated by considering the effects of points in the fuel grid (in the order ignited) on surrounding points.

The effect of each burning point on its neighbours is determined by an elliptically shaped template that represents the area of scorch around a burning point at its focus (Green, 1983). When any point in the fuel array is ignited, the ignition template is placed over the fuel array with its centre above the newly-ignited point. Entries in the template determine the effect that the ignited point has on nearby fuel elements; points not lying under the template are assumed to be unaffected by the burning fuel element.

If fuel is packed more sparsely in the fuel bed, then a burning point source would scorch fewer points of fuel around it. Hence, in the model, sparser fuel distributions are modelled by reducing the size  $M$  of the ignition template ( $M$  is the number of cells on the template's longest radius). The final shape produced by the model is approximately an ellipse when a large template is used. Several fire-spread mechanisms can be simulated by the model (Green, 1983).

## METHODS

### *The experimental data*

Maps of experimental fires burning in eucalypt and grassy fuels were provided for analysis by G.B. Peet and N.P. Cheney respectively. In both data sets, the maps consisted of contours (Fig. 1a) marking out the areal extent of fires at progressive times after ignition for periods up to 40

TABLE I

Recorded windspeeds for the experimental fires (m/s)

Data <sup>1</sup> set	Mean	S.D.	Max.	Min.	Correlation with time	Trends with time <sup>2</sup>		
						(2) > (1)	(3) > (1)	(3) > (2)
Peet	1.14	0.38	2.01	0.54	-0.085	7	7	5
Cheney	1.31	0.47	2.34	0.46	-0.029	5	6	8

<sup>1</sup> Windspeed data was available for only 9 of Peet's fires (27 contours).<sup>2</sup> The figures tabulated are the numbers of fires for which the contour at time (2) had a greater windspeed recorded than at time (1), etc.

minutes. Only those fires showing approximately bilateral symmetry about their major axes, and with the ignition point lying on or close to the major axis, were selected for analysis; we assumed that either fuel, terrain, or wind were not uniform in the other fires. Fires for which wind direction (as indicated by the changing orientation of the major axis) had varied substantially during the course of the burn were also excluded. In all, 20 fires and a total of 60 contours were analyzed.

The maps were digitized using a Tektronix 4954 digitizing table. Each contour (Fig. 1a) was expressed as a set of polar coordinates, with the ignition point as origin, and with angles measured clockwise from the major axis (downwind) at 5° intervals. To simplify the curve-fitting procedures, values of  $X$  (Fig. 1a) were scaled to make the maximum value one for each contour.

The range of prevailing windspeeds for the fires considered was very small (Table I). Trends in the values of model parameters with changing windspeed were thus unclear in some cases, and even where significant correlations were found, it was impossible to determine what sort of regression model best fitted the trends. For both data sets, the prevailing windspeeds increased during the course of most fires (Table I). These increasing trends may have been accidental or may have been a consequence of the fires themselves. In either case they affect conclusions about parameter trends through time.

#### *Fitting shapes to the experimental data*

For each contour, curves-of-best-fit were found for each model. The "curve-of-best-fit" is the shape that has the maximum coefficient-of-determination  $r^2$  with respect to the experimental data, defined by

$$r^2 = 1 - \sum_{\theta} (S(\theta) - X(\theta))^2 / \text{var}(X)$$

where  $S(\theta)$  and  $X(\theta)$  denote distances from the ignition point  $I$  of points on

the fitted and experimental curves respectively (Fig. 1a, 1b) and  $\text{var}(X)$  is the variance of distances from the ignition point to the experimental curve.

We performed two tests to check the digitizing and model-fitting procedures. In the first we digitized a perfect ellipse, and similarly perfect examples of each of the other shapes being considered, and applied the curve-fitting procedure. In the second we compared the results of repeatedly digitizing a single fire contour and applying the curve-fitting procedure each time.

Associated with each fire-spread model were parameters that fixed the size, shape, and position of the resulting curve relative to the ignition point and perimeter of an experimental fire. The parameter values that fix the "curve-of-best-fit" were found using a "hill-climbing" algorithm. That is, initial estimates (assumed to be close to the final values) for each parameter were systematically changed by small amounts until a combination was found that maximized  $r^2$ . The parameters used and their initial estimates were as follows.

(1) *Ellipse*

The polar equation of an ellipse with the origin at its focus (Fig. 1b) is

$$R = L(1 - e^2)/(1 - e \cos \psi)$$

where  $R$  = distance from the focus,  $L$  = length of major axis,  $e$  = eccentricity,  $\psi$  = angle from the major axis.

Estimates of the initial values of three parameters were needed:

(a) The length  $L$  of the major axis (Fig. 1a) was estimated to be

$$L = X(0) + X(180).$$

(b) The estimate for  $e$  was

$$e = (1 - A/L)^{1/2}$$

where  $A$  is the length of the minor axis (Fig. 1c); the maximum width of the fire (perpendicular to the wind direction) was used as an initial estimate for  $A$ .

(c) Since the digitized contours were expressed in polar coordinates based on an origin at the point of ignition of the fire, the distance  $d$  separating the focus from the ignition point I (Fig. 1b) was estimated to be

$$d = eL - X(\theta_m) \cos \theta_m,$$

where  $\theta_m$  is the angle subtended by the major axis and the line joining I to the end of the minor axis.

Polar coordinates  $(\theta, S(\theta))$  of the fitted ellipse relative to the ignition

point were then computed using the equations

$$S^2 = R^2 + 2 R d \cos \psi + d^2$$

$$\theta = \arccos((R \cos \psi + d)/S)$$

### (2) Double Ellipse

The double ellipse (Fig. 1c) was fitted in similar fashion to the ellipse except that different parameters were needed for the headfire and backfire shapes (with the two shapes interlocking at the minor axis). Four parameters were therefore needed, with the values they took for the fitted ellipse being used as initial estimates. (a) The length  $A$  of the minor axis (Fig. 1c); (b) The distance  $m$  along the major axis from the ignition point to the minor axis (Fig. 1c); (c) The eccentricity  $e_1$  of the headfire ellipse; (d) The eccentricity  $e_2$  of the backfire ellipse.

Note that the double ellipse can assume both elliptical and ovoid forms: if the eccentricities of the headfire and backfire ellipses forming the double ellipse are equal, then the overall shape is a single ellipse; if the eccentricities are different, then the overall shape approximates an ovoid.

### (3) Ovoid

Equation 1 can be rewritten in the form

$$pR + R' = Q/e$$

where  $p$  is the “pointedness” factor,  $Q$  is the separation of the foci  $F$  and  $F'$  (Fig. 1d), and  $e$  is the eccentricity. If  $p = 1$  then the ovoid reduces to an ellipse.

For  $p > 1$ , the polar equation of an ovoid is

$$R = \frac{Q}{e(p^2 - 1)} \left( p - e \cos \theta + \left( (p - e \cos \theta)^2 - (p^2 - 1)(1 - e^2) \right)^{1/2} \right)$$

The ovoid (Fig. 1d) is fixed by the four parameters  $p$ ,  $Q$ ,  $e$ , and  $d$ , initially estimated as follows:

$$p = (X(180) + X(0)) / (X(180) - X(0))$$

$$Q = (p + 1)(X(180) - X(0)) / 2$$

$$e = 2Q / (p + 1)L$$

The separation  $d$  of focus and ignition point was initially estimated to be zero. The resulting ovoid was constrained to be non-elliptical and to attain its greatest width nearer the ignition point than the second focus ( $p > 1$ ).

#### (4) *Rectangle*

A rectangle was fitted to each experimental fire shape by taking the major axis to be the y-axis of a cartesian coordinate system with origin at the ignition point (Fig. 1e). The rectangle-of-best-fit was determined by three parameters  $X_1$ ,  $Y_1$ ,  $Y_2$  representing the perpendicular distances of the sides from the ignition point. These distances were initially set to be the maximum distances (along the axes) from I of points on the experimental curve. Note that the rectangle was constrained to be symmetric about the major axis since all of the other models being tested had this symmetry.

#### (5) *Simulation*

The simulation (Fig. 1f) needed four parameters: (a) The eccentricity  $e$  of the elliptical template—the eccentricity of the fitted ellipse was used as an initial estimate. (b) Since distances in the simulation model were measured in numbers of cells, while the experimental data was standardized to be less than one, a scaling factor  $w$  was needed to achieve correspondence between the two sets of measurements. This factor was initially estimated to be the reciprocal of the number of cells lying on the major axis of the simulated fire. (c) The template size  $M$  was initially set at the maximum possible value ( $M = 24$ ). (d) Zero was used as an initial estimate of the focus/ignition separation  $d$ .

The simulations required large amounts of computer time, so it was not feasible to test for the combination of fire-spread rules that gave the best possible curve fit. Only the “inverse contact” model (Green, 1983) was tested: this version of the model assumes that heat dissipated as the inverse of distance from a burning point in the fuel array and that the time at which any given fuel element ignited was determined by its earliest contact with heat from the fire.

#### *Parameter trends*

Values of the shape parameters that gave the best fits of each model to the experimental data were examined for trends with time and with changing windspeed. These trends were assessed by computing correlation coefficients between realized values of the parameter concerned and time or windspeed. Since conditions that influence parameter values, but were not recorded in the data, were likely to vary considerably between fires, trends in parameter values were more reliably assessed by comparing with each other the values found for a parameter at each of the three times tested for a given fire. The total number of fires in each data set for which the parameter took higher values at the second and third times tested than at the first and second times were recorded. The sign test was used to determine whether the totals recorded differed significantly from the numbers expected by chance.



## RESULTS AND DISCUSSION

*Goodness-of-fit comparisons*

Fitting the five models to digitized maps of each other highlighted the importance of flexibility in the fitting process: the double ellipse and the ovoid (which had the most shape parameters) gave better fits to the other models than those other models did to themselves. Also, because of inaccuracies in the digitizing process, no model achieved a correlation of 1 when fitted to a digitized map of itself. Multiple test runs on a single contour showed that a standard error of about one percent could be expected in goodness of fit and in parameter estimates because of the digitizing process.

Fits of all the models, even the rectangle, gave extremely high coefficients of determination to Cheney's fire maps (Table II). Overall, the ellipse and double ellipse gave better fits to these fires than the other models. Since the eccentricities of the two sections of the double ellipse were virtually identical for most of Cheney's fire maps (that is the curve-of-best-fit was an ellipse), we conclude that the ellipse gave the closest fits to the shapes of Cheney's fires. All of the models gave better fits than the rectangle to most (or all) fires.

TABLE II

Coefficients of determination for model fits to the fire maps ( $n = 30$  for each data set)

	Ellipse	Double ellipse	Ovoid	Rectangle	Simulation
<i>Peet's fires</i>					
Mean $r^2$	0.910	0.914	0.917	0.792	0.833
S.D.	0.123	0.122	0.112	0.179	0.197
No. of times <sup>1</sup> best model	4	10	16	0	1
No. of times <sup>2</sup> better than rectangle	30***	30***	30***	—	24***
<i>Cheney's fires</i>					
Mean $r^2$	0.976	0.978	0.960	0.936	0.945
S.D.	0.021	0.020	0.038	0.023	0.077
No. of times <sup>1</sup> best model	11	24	5	0	0
No. of times <sup>2</sup> better than rectangle	30***	30***	25**	—	23*

<sup>1</sup> In many cases, two or more models tied for the highest coefficient of determination.

<sup>2</sup> Significance is determined by a sign test, with 15 the number expected by chance.

Fits of all of the models gave substantially lower coefficients of determination to Peet's fire maps (Table II) than to Cheney's maps. Many of the contours tested from Peet's fires were less regular than contours of Cheney's fires, apparently because irregularities in fuel distribution and wind direction had greater effect on the smaller fires. Overall, the ovoid gave the best fits to Peet's fires—as Peet himself concluded (Peet, 1967). On this data set, the two halves of the double ellipse usually had different eccentricities, so the model was approximating the ovoid more than the ellipse.

The results indicate that the simulation model is less adequate at predicting fire spread than the continuous models tested. The contours of simulated fires changed only in discrete amounts, posing serious problems for the “hill-climbing” algorithm. Small changes of  $e$  or  $M$  towards their optimum values sometimes produced no change in the simulated shape, thus halting the search for the curve-of-best-fit too early. Also, just one combination of fire-spread rules was tested; trials showed that other combinations performed better on at least some contours. While more exhaustive testing may have produced results as good as those of the continuous models, the simulation model is not practical for fire prediction because of the massive amounts of computer time required. It must be emphasized, however, that this conclusion in no way invalidates it as a tool for understanding fire-spread mechanisms.

### *Parameter trends*

Eccentricity (Table III) showed very clear patterns for all of the models (for the rectangle, both the eccentricity of the inscribed ellipse and the length/breadth ratio were used), and in all models was higher for Cheney's fires than for Peet's. The eccentricity parameter for all models had a significant positive correlation with windspeed (higher windspeeds produce longer fires). It was significantly correlated with time for Cheney's fires only, but increased with time during fires in both data sets (a sign test gave  $P = 0.03$ ). Not all of the correlation of eccentricity with time can be accounted for by the windspeed trends through time, since for Cheney's data the joint correlation of eccentricity on linear combinations of windspeed and time was higher than the correlation with either variable alone.

The average pointedness of the ovoids fitted to Cheney's fires was only slightly greater than one (Table IV), supporting the earlier conclusion that the ellipse is the best model for Cheney's fires. Ovoids fitted to the experimental data tended to become less pointed with time ( $p$  decreased), though the trend was significant for Peet's data only. That is, although fires may start as ovoids, they become more elliptical in shape as they grow. This trend agrees with predictions of the simulation model about shape changes in a

TABLE III

Trends in eccentricity for fits of models to experimental data

Test	Ellipse	Double ellipse		Ovoid	Rectangle <sup>1</sup>		Simulation
		Back	Head		(a)	(b)	
Means and standard deviations							
Peet							
Mean	0.578	0.598	0.581	0.482	0.607	1.242	0.502
S.D.	0.216	0.221	0.246	0.196	0.187	0.413	0.202
Cheney							
Mean	0.851	0.851	0.855	0.822	0.865	2.348	0.827
S.D.	0.097	0.099	0.101	0.128	0.099	0.705	0.099
Correlations of e with							
Windspeed							
Peet (n = 27)	0.576**	0.308*	0.544**	0.684**	0.614**	0.458**	0.458**
Cheney (n = 30)	0.523**	0.549**	0.475**	0.473**	0.494**	0.552**	0.551**
Time							
Peet (n = 27)	-0.029	0.048	-0.057	-0.062	-0.036	0.023	0.169
Cheney (n = 30)	0.461**	0.427**	0.466**	0.353*	0.442**	0.495**	0.301*
Time trends							
Peet (n = 9)							
(2) > (1)	7	6	6	6	5	6	7
(3) > (1)	7	8	7	7	7	8	8
(3) > (2)	7	6	8	6	6	7	8
Cheney (n = 10)							
(2) > (1)	7	7	7	8	7	7	8
(3) > (1)	8	8	9	8	8	8	7
(3) > (2)	8	8	7	7	8	8	8

<sup>1</sup> Two measures of eccentricity were tested for the rectangle: (a) The eccentricity of an ellipse inscribed within the rectangle. (b) The length/breadth ratio of the rectangle. The entries for (2) > (1) denote the number of fires for which the eccentricity of the curve fitted to the contour at time (2) was greater than at time (1), etc.

TABLE IV

Pattern in the pointedness parameter for ovoids fitted to experimental fire maps

Data	Mean <sup>1</sup>	Correlations with:			Trends with time <sup>2</sup>		
		<i>e</i> (ovoid)	Wind	Time	(2) < (1)	(3) < (1)	(3) < (2)
Peet	2.19	-0.727**	-0.394**	0.110	7	9	7
Cheney	1.21	-0.822**	-0.421**	-0.079	7	7	6

<sup>1</sup> The pointedness was constrained to exceed one.<sup>2</sup> The figures tabulated are the numbers of fires (out of 10) for which the pointedness of the ovoid fitted to the contour at time (2) was less than at time (1), etc.

growing fire (Green, 1983). The strong negative correlation between  $p$  and  $e$  on both data sets may be an artefact of the curve-fitting process. If it is, then the negative correlation between  $p$  and windspeed would simply reflect the correlation between  $e$  and windspeed.

Few trends are apparent in the values obtained for other parameters; in the case of parameters relating to size, this occurs because of standardizing the experimental data. For all models except the ovoid, 21 or more of the 30 contours in each data set yielded positive separations between the ignition point and the fitted focus (a sign test gave  $P < 0.0001$  for this result). The ovoid scored exactly at the chance level on Peet's fires and had a significant number of contours with negative separations on Cheney's data. The results imply that the focus of most fitted models tended to lie downwind of the ignition point. For the ovoid, however, the pointedness parameter probably made the separation unnecessary. There were no significant correlations between the focus/ignition separation and either time or windspeed.

In all cases, the ignition template used by the simulation of best fit had size  $M$  equal or close to 24. Since the experimental burns were conducted in essentially continuous fuel beds, such a pattern was to be expected.

## CONCLUSIONS

Our results demonstrate that all five models of fire shape tested here (even the rectangle), provide reasonable approximations of the fire contours examined. More importantly, the shape parameters for all models showed significant correlations with environmental parameters and consistent variations between the two data sets and through time. The number of parameters used to fix the shapes, rather than intrinsic properties of the shapes themselves, appears to be the chief determinant of how good a fit can be achieved to real fire maps.

These conclusions are based on data from a number of fires in two different fuel types, but over a very limited range of low wind velocities and

rates of spread. The results may be quite different for fires subject to higher wind velocities or higher rates of spread.

We feel that, because of the mathematical flexibility of the models used to describe fire shapes, little further understanding of the process involved in fire spread will be made by attempting to fit more complicated models to observed fire shapes. Controlled laboratory experiments and micro-meteorological measurements made at the fire front will prove much more helpful.

#### ACKNOWLEDGEMENTS

We are grateful to George Peet and to Phil Cheney for kindly making their experimental fire data available to us.

#### REFERENCES

- Albini, F.A., 1976. Estimating wildfire behaviour and effects. USDA For. Serv. Gen. Tech. Rep., INT-30, Washington, DC.
- Anderson, D.H., Catchpole, E.A., de Mestre, N.J. and Parkes, T., 1982. Modelling the spread of grass fires. *J. Aust. Math. Soc., Series B*, 23: 451-466.
- Frandsen, W.H., 1974. A fire-spread model for spatially non-uniform forest fuel arrays. West States Section, The Combustion Institute, Northridge, CA, 35 pp.
- Frandsen, W.H. and Andrews, P.L., 1979. Fire behaviour in nonuniform fuels. USDA For. Serv. Res. Paper INT-232, Washington, DC.
- Green, D.G., 1983. Simulated fire-spread in discrete fuels. *Ecol. Modelling*, 20: 21-32.
- Kourtz, P.H. and O'Regan, W.G., 1971. Model for a small forest fire...to simulate burned and burning areas for use in a detection model. *For. Sci.*, 17: 163-169.
- McArthur, A.G., 1962. Control burning in eucalypt forests. Commonwealth of Australia Forestry and Timber Bureau, Leaflet No. 80, Canberra.
- McArthur, A.G., 1966. Weather and grassland fire behaviour. Commonwealth of Australia Forestry and Timber Bureau, Leaflet No. 100.
- Noble, I.R., Bary, G.A.V. and Gill, A.M., 1980. McArthur's fire danger meters expressed as equations. *Aust. J. Ecol.*, 5: 201-203.
- Peet, G.B., 1967. The shape of mild fires in jarrah forest. *Aust. For.*, 31: 121-127.
- Rothermel, R.C., 1972. A mathematical model for predicting fire-spread in wildland fuels. USDA For. Serv. Res. Paper INT-115, Washington, DC.
- Sneeuwjagt, R.J. and Peet, G.B., 1979. Forest fire behaviour tables for Western Australia. West Australian Forest Department, Perth.
- Sussman, M.H., 1966. Maxwell's ovals and the refraction of light, *Am. J. Phys.*, 34: 416-418.
- Valendik, E.N., Vorobyev, O.B. and Matveev, A.M., 1977. Predicting patterns of perimeter increase in forest fires by computer simulation. In: *Characteristics of Combustion Processes in the Forest*, Institut Lesa i Drevesiny, 52-66 (in Russian).
- Van Wagner, C.E., 1969. A simple fire-growth model. *For. Chron.*, 45(2): 103-104.